Microfluid Nanofluid (2008) 5:733–740
DOI 10.1007/s10404-008-0309-1

SHORT COMMUNICATION

Flow rate-modified streaming effects in heterogeneous microchannels

Junjie Zhu · Christian Davidson · Xiangchun Xuan

Received: 26 March 2008 / Accepted: 19 May 2008 / Published online: 3 June 2008

Abstract A general model based on the Onsager reciprocal relations is developed to study the streaming potential and streaming current in heterogeneous microchannels. The surface heterogeneities may be symmetrically or asymmetrically distributed parallel or perpendicular to the flow axis. Both streaming effects are modified by the flow rate through the heterogeneous channel, to eliminate the possible influence of electrokinetic flow on the streaming potential and streaming current measurements. Although they are still dependent on the distribution of surface heterogeneity, the flow rate-modified streaming effects are demonstrated to provide more consistent results with the traditional linear assumption than do the traditional ones, especially apparent in small microchannels.

Keywords Streaming potential · Streaming current · Heterogeneous microchannel · Onsager reciprocal relations · Flow rate

List of symbols

c_b	ionic concentration
e	charge of proton
F_i	defined nondimensional functions ($i = 1, 2, 3$)
G	hydrodynamic conductance
h	half channel height
j	electrical current density
I	electrical current
k_B	Boltzmann's constant
K	nondimensional channel height
l	channel length
M	phenomenological coefficient
N_A	Avogadro's number
p	hydrodynamic pressure
$\hat{q}$	direction of surface charge variations
Q	fluid volume flow rate
R	universal gas constant
S	electrical conductance
T	liquid temperature
u	fluid velocity
w	channel width
y	transverse coordinate
Z	figure of merit
z_v	valence of electrolyte ions

Greek symbols

β	nondimensional property of fluid (Levine number)
η	normalized y coordinate
ε	fluid permittivity
ϕ	electrical potential
κ	Debye–Huckel parameter
Λ	molar conductivity of fluid
μ	fluid viscosity
ψ	electrical double-layer potential
Ψ	normalized double-layer potential
Ψ_0	double-layer potential at channel center
ζ	zeta potential
$\zeta_\pm$	zeta potentials at the top and bottom walls
ζ^*	normalized zeta potential
$\zeta^*_\pm$	normalized zeta potentials at the top and bottom walls
$\langle\zeta\rangle^*$	average zeta potential of the two channel walls
ζ^*_D	discrepancy of the zeta potentials of the two channel walls

J. Zhu · C. Davidson · X. Xuan (✉)
Department of Mechanical Engineering,
Clemson University, Clemson, SC 29634-0921, USA
e-mail: xcxuan@clemson.edu

Subscripts

i the ith section of a heterogeneous microchannel
Q flow rate-modified
sp streaming potential
sc streaming current
$\perp$ $\hat{q} \perp \nabla p$
$\parallel$ $\hat{q} \parallel \nabla p$

1 Introduction

Heterogeneities on channel surfaces may arise due to solute adsorption (Towns and Regnier 1992; Zembala and Adamczyk 2000), chemical coating (Towns and Regnier 1991), and various other reasons (Zembala 2004). These heterogeneities, which typically exhibit different surface charges or zeta potentials from that of the original surface, may be characterized by monitoring the streaming potential (Norde and Rouwendal 1990; Elgersma et al. 1992; Werner et al. 1999) or streaming current (Werner et al. 1998) when a fluid is forced to flow past the surface. It is generally assumed that the change in these streaming effects is proportional to the change in surface charges (Hunter 1981; Anderson and Idol 1985). This linear assumption, however, is only valid in large channels with negligible double-layer overlapping, i.e., thin double-layer approximation (Brunet and Ajdari 2006). In small channels, Erickson and Li (2001) demonstrated through numerical simulations that streaming potential measurements may deviate significantly from the linear prediction when the stripwise heterogeneities are parallel to the flow axis. In the same situation, streaming current measurements were found to provide more consistent results. These phenomena were attributed to the streaming potential-induced flow impedance, i.e., electroviscous effects (Li 2001, 2004), which vanishes in the streaming current case.

Other than those referred above, a number of other studies on electrokinetic streaming effects in heterogeneous microchannels have been reviewed in our earlier paper (Xuan 2008) and thus omitted here. The majority of these works solved simultaneously the Navier–Stokes and Poisson–Nernst–Planck equations, the result of which is the availability of flow behavior adjacent to surface heterogeneities other than the streaming effects. However, the true factors affecting the streaming processes were often hidden in the complicated simulations. In a recent work, we developed an analytical model based on the Onsager reciprocal relations (de Groot 1952) to study the streaming potential and electroviscous effects in microchannels with surface heterogeneities either parallel or perpendicular to the flow axis (Xuan 2008). It was found that streaming potential varies not only with the degree but also with the arrangement of surface heterogeneity, especially apparent in small channels. In this article, the Onsager relations-based analytical model is generalized to study both the streaming potential and the streaming current to complete the topic on electrokinetic streaming effects in heterogeneous microchannels. These heterogeneities may be symmetrically or asymmetrically distributed parallel or perpendicular to the flow axis. Moreover, flow rate-modified streaming effects are defined to eliminate the aforementioned influence of electrokinetic flow on the streaming potential and streaming current measurements.

It is also noticed that lots of work have been done on the influence of surface heterogeneity on electroosmotic flow in microchannels, which is of great interest to electrokinetic microfluidics-based applications (Li 2004; Squires and Quake 2005). Here, we refer to just a few of the representative papers and more related ones were cited therein. Assuming a very thin double layer, Anderson and Idol (1985) first considered the electroosmosis through pores with nonuniformly charged walls that displays flow separation and circulation. Their method was then extended by Ajdari (1995, 1996) to analyze the effects of charge and shape modulations on electroosmotic flow between two parallel plates. The predicted flow behavior was later verified experimentally by Stroock et al. (2000) in slit microchannels with patterned surface charges. With a caged-dye-based velocimetry, Herr et al. (2000) recently observed in a hybrid capillary with nonuniform zeta potentials, significant deviations in electroosmotic velocity from the typical plug-like profile. More recently, Erickson and Li (2002) proposed the use of surface heterogeneity to enhance species-mixing, which was later implemented by Biddiss et al. (2004) in a T-channel.

In addition, we would like to point out that the thermo-electro-hydrodynamic approach presented herein has also been applied to the analyses of electroosmotic flow in heterogeneous microchannels (Xuan and Li 2004), electrokinetic flow control in microfluidic networks (Berli 2007, 2008), and electrokinetic energy conversion in nanofluidic channels (Xuan and Li 2006; van der Heyden et al. 2006; Chein and Liao 2007; Davidson and Xuan 2008a, b; Ren and Stein 2008).

2 Thermodynamic analysis

Two patterns of surface heterogeneities in slit microchannels are examined here, namely $\hat{q} \parallel \nabla p$ or $\hat{q} \perp \nabla p$, indicating that the direction of surface charge variations, $\hat{q}$, may be parallel or perpendicular to the applied pressure gradient (i.e., the flow direction), ∇p. As sketched in Fig. 1, the heterogeneous microchannel may be conveniently divided into n sections. Within every section, the zeta potential of each wall is uniform but may be identical

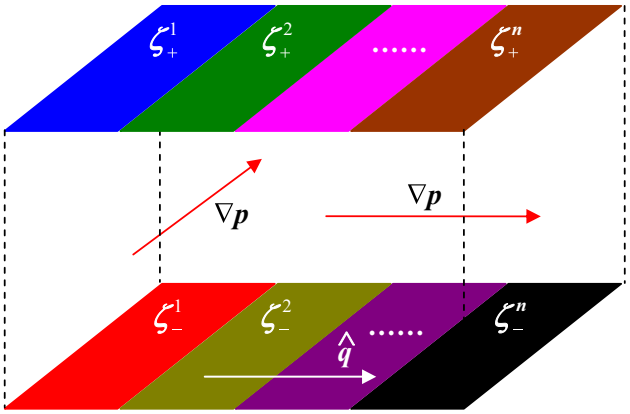

Fig. 1 Scheme of heterogeneous microchannels with $\hat{q} \parallel \nabla p$ or $\hat{q} \perp \nabla p$, where $\hat{q}$ denotes the direction of surface charge variations and ∇p indicates the applied pressure gradient (i.e., the flow direction)

or dissimilar to each other. Namely, the heterogeneities may be symmetrically or asymmetrically arranged in the two walls (Erickson and Li 2001). The flow transition regions near the surface charge discontinuities and the end reservoirs are neglected. In other words, fluid flow is assumed fully developed in each section. This assumption has been demonstrated reasonable in a number of recent studies, unless the length of a section is smaller than or comparable to the characteristic dimension of its cross-section (Ren and Li 2001; Xuan and Li 2004; Berli 2007).

In each of the n sections sketched in Fig. 1, the Onsager reciprocal relations (Brunet and Ajdari 2004) apply, i.e.,

$$Q_i = G_i(-\Delta p)_i + M_i(-\Delta\phi)_i \tag{1}$$

$$I_i = M_i(-\Delta p)_i + S_i(-\Delta\phi)_i \tag{2}$$

where the "fluxes" are volumetric flow-rate, Q, and electrical current, I, while the corresponding "forces" are pressure difference, Δp, and electrical potential difference, $\Delta\phi$, in each section. The subindex i indicates the ith section of the heterogeneous channel. Additionally, G indicates the hydrodynamic conductance, M characterizes the electro-osmotic and streaming effects, and S indicates the electrical conductance. These phenomenological coefficients may be specified through a routine electrokinetic flow analysis as presented in the next section.

2.1 $\hat{q} \parallel \nabla p$

In a channel with $\hat{q} \parallel \nabla p$ (see Fig. 1), the fluid and electrical current both flow in series through the n sections and hence should be continuous through the entire channel ($i = 1 \ldots n$)

$$Q_{\parallel} = G_i(-\Delta p)_i + M_i(-\Delta\phi)_i \tag{3}$$

$$I_{\parallel} = M_i(-\Delta p)_i + S_i(-\Delta\phi)_i \tag{4}$$

where the subscript $\parallel$ indicates the case with $\hat{q} \parallel \nabla p$. In the streaming potential measurements (indicated by the subscript "sp"), there is no net current through each section of the heterogeneous channel, i.e., $I_{\parallel} = I_i = 0$ (see also Eq. 2), so that one obtains

$$\phi_{\mathrm{sp},\parallel} = \sum_{i=1}^{n} (\Delta\phi)_i = \frac{\sum_{i=1}^{n} \frac{Z_i}{M_i(1-Z_i)}}{\sum_{i=1}^{n} \frac{1}{G_i(1-Z_i)}}(-\Delta p) \tag{5}$$

where $Z_i = M_i^2/G_iS_i$ is previously termed "figure of merit," as it gauges the performance of electrokinetic energy conversion (Morrison and Osterle 1965; Xuan and Li 2006). The flow rate in this situation is expressed as

$$Q_{\mathrm{sp},\parallel} = \frac{1}{\sum_{i=1}^{n} \frac{1}{G_i(1-Z_i)}}(-\Delta p) \tag{6}$$

Dividing Eq. 5 by the flow rate in Eq. 6 yields the flow rate-modified streaming potential

$$\phi_{\mathrm{Q},\parallel} = \phi_{\mathrm{sp},\parallel} \Big/ Q_{\mathrm{sp},\parallel} = \sum_{i=1}^{n} \frac{Z_i}{M_i(1-Z_i)} = \sum_{i=1}^{n} \frac{M_i/S_i}{G_i(1-Z_i)} = \sum_{i=1}^{n} \phi_{\mathrm{Q},i} \tag{7}$$

where $\phi_{Q,i} = M_i/S_i/G_i(1 - Z_i)$ is exactly the flow rate-modified streaming potential in the ith section. Therefore, the flow rate-modified streaming potential in an n-section heterogeneous microchannel with $\hat{q} \parallel \nabla p$ is simply given by the summation of that in each section.

In the streaming current measurements (indicated by the subscript "sc"), there is no potential difference between the two ends of the heterogeneous channel, i.e., $\sum_{i=1}^{n} (\Delta\phi)_i = 0$, yielding

$$I_{\mathrm{sc},\parallel} = \frac{\sum_{i=1}^{n} \frac{Z_i}{M_i(1-Z_i)}}{\sum_{i=1}^{n} \frac{1}{S_i(1-Z_i)} \sum_{i=1}^{n} \frac{1}{G_i(1-Z_i)} - \left(\sum_{i=1}^{n} \frac{Z_i}{M_i(1-Z_i)}\right)^2}(-\Delta p) \tag{8}$$

The flow rate is given by

$$Q_{\mathrm{sc},\parallel} = \frac{\sum_{i=1}^{n} \frac{1}{S_i(1-Z_i)}}{\sum_{i=1}^{n} \frac{1}{S_i(1-Z_i)} \sum_{i=1}^{n} \frac{1}{G_i(1-Z_i)} - \left(\sum_{i=1}^{n} \frac{Z_i}{M_i(1-Z_i)}\right)^2}(-\Delta p) \tag{9}$$

Thus, the flow rate-modified streaming current is written as

$$I_{\mathrm{Q},\parallel} = I_{\mathrm{sc},\parallel} \Big/ Q_{\mathrm{sc},\parallel} = \frac{\sum_{i=1}^{n} \frac{Z_i}{M_i(1-Z_i)}}{\sum_{i=1}^{n} \frac{1}{S_i(1-Z_i)}} = \frac{\sum_{i=1}^{n} \frac{M_i}{G_i} \frac{1}{S_i(1-Z_i)}}{\sum_{i=1}^{n} \frac{1}{S_i(1-Z_i)}} = \frac{\sum_{i=1}^{n} I_{\mathrm{Q},i} S_{\mathrm{EK},i}}{\sum_{i=1}^{n} S_{\mathrm{EK},i}} \tag{10}$$

where $I_{\mathrm{Q},i} = M_i/G_i$ is the flow rate-modified streaming current in the ith section, and $S_{\mathrm{EK},i} = 1/S_i(1 - Z_i)$ may be

termed "electrokinetic conductance." Therefore, the flow rate-modified streaming current in an n-section heterogeneous microchannel with $\hat{q} \parallel \nabla p$ is the weighted average of that in each section whose "electrokinetic conductance" serves as the weighting factor.

2.2 $\hat{q} \perp \nabla p$

In a channel with $\hat{q} \perp \nabla p$ (see Fig. 1), the fluid and electrical current both flow in parallel through the n sections, i.e.,

$$Q_{\perp} = \sum_{i=1}^{n} G_i(-\Delta p) + \sum_{i=1}^{n} M_i(-\Delta\phi) \tag{11}$$

$$I_{\perp} = \sum_{i=1}^{n} M_i(-\Delta p) + \sum_{i=1}^{n} S_i(-\Delta\phi) \tag{12}$$

where the subscript $\perp$ indicates the case of $\hat{q} \perp \nabla p$. In the streaming potential measurements, the zero current condition through the heterogeneous channel produces

$$\phi_{\mathrm{sp},\perp} = \frac{\sum_{i=1}^{n} M_i}{\sum_{i=1}^{n} S_i}(-\Delta p) \tag{13}$$

As the flow rate is

$$Q_{\mathrm{sp},\perp} = \sum_{i=1}^{n} G_i(1 - Z_{\perp})(-\Delta p) \tag{14}$$

the flow rate-modified streaming potential is thus expressed as

$$\phi_{\mathrm{Q},\perp} = \phi_{\mathrm{sp},\perp}/Q_{\mathrm{sp},\perp} = \frac{Z_{\perp}}{\sum_{i=1}^{n} M_i(1 - Z_{\perp})} \tag{15}$$

where $Z_{\perp} = \left(\sum_{i=1}^{n} M_i\right)^2 \Big/ \sum_{i=1}^{n} G_i \sum_{i=1}^{n} S_i$ can be viewed as the overall "figure of merit" of the heterogeneous channel. Of note here is that Eq. 15 holds a similar functional form to that in a channel with $\hat{q} \parallel \nabla p$ (refer to Eq. 7).

In the streaming current measurements, the zero potential difference between the two ends of each section of the heterogeneous channel leads to an accumulated streaming current

$$I_{\mathrm{sc},\perp} = \sum_{i=1}^{n} M_i(-\Delta p) \tag{16}$$

Considering the flow rate in this situation

$$Q_{\mathrm{sc},\perp} = \sum_{i=1}^{n} G_i(-\Delta p) \tag{17}$$

one can write the flow rate-modified streaming current as

$$I_{\mathrm{Q},\perp} = I_{\mathrm{sc},\perp}/Q_{\mathrm{sc},\perp} = \frac{\sum_{i=1}^{n} M_i}{\sum_{i=1}^{n} G_i} \tag{18}$$

3 Electrokinetic flow analysis

In this section, the phenomenological coefficients G, M, and S are determined from the electrokinetic flow analysis. For generality, consider a combined pressure-driven and electroosmotic flow in a slit channel with dissimilar zeta potentials on its two walls. The fully developed fluid velocity parallel to the flow axis, u, is derived as

$$u = \frac{h^2}{2\mu}\left(1 - \frac{y^2}{h^2}\right)\frac{(-\Delta p)}{l} + \frac{\varepsilon}{\mu}\left(\psi - \frac{\zeta_+ - \zeta_-}{2h}y - \frac{\zeta_+ + \zeta_-}{2}\right)\frac{(-\Delta\varphi)}{l} \tag{19}$$

where h is the half channel height, μ the fluid viscosity, y the transverse coordinate originating from the channel axis, l the channel length, ε the fluid permittivity, ψ the electrical double-layer potential, and ζ_+ and ζ_- the zeta potentials of the top ($y = +h$) and bottom ($y = -h$) walls. The electrical current density, j, is given by (Hunter 1981; Li 2004)

$$j = -\varepsilon\frac{d^2\psi}{dy^2}u + c_{\mathrm{b}}\Lambda\cosh\left(\frac{z_{\mathrm{v}}e\psi}{k_{\mathrm{B}}T}\right)\frac{(-\Delta\phi)}{l} \tag{20}$$

where c_b is the ionic concentration of the bulk electrolyte, Λ the bulk molar conductivity, z_{v} the valence of electrolyte ions (assumed symmetric here for simplicity), e the charge of a proton, k_{B} the Boltzmann's constant, and T the absolute fluid temperature.

Integrating Eqs. 19 and 20 over the channel cross-section and then comparing them with Eqs. 1 and 2 (with the subindices i dropped), one can obtain

$$G = \frac{2h^3 w}{3\mu l} \tag{21}$$

$$M = \frac{\varepsilon h w}{\mu l}\frac{k_{\mathrm{B}}T}{z_v e}(F_1 - 2\langle\zeta\rangle^*) \tag{22}$$

$$S = \frac{\varepsilon^2 w}{\mu h l}\left(\frac{k_{\mathrm{B}}T}{z_v e}\right)^2\left(F_2 - 2\zeta_{\mathrm{D}}^{*2} + \beta K^2 F_3\right) \tag{23}$$

$$F_1 = \int_{-1}^{1} \Psi \mathrm{d}\eta, \quad F_2 = \int_{-1}^{1} (\mathrm{d}\Psi/\mathrm{d}\eta)^2 \mathrm{d}\eta, \quad F_3 = \int_{-1}^{1} \cosh(\Psi)\mathrm{d}\eta \tag{24}$$

where w is the channel width, $\Psi = z_v e\psi/k_{\mathrm{B}}T$ the normalized double-layer potential, $\eta = y/h$ the normalized y coordinate. Four other dimensionless parameters are involved in the

definitions of phenomenological coefficients: $\langle\zeta\rangle^* = z_v e(\zeta_+ + \zeta_-)/2k_BT$ and $\zeta_D^* = z_v e(\zeta_+ - \zeta_-)/2k_BT$ are the average and the discrepancy of the zeta potentials of the two walls; $\beta = \Lambda\mu/\varepsilon RT$ [previously termed Levine number by Griffiths and Nilson (2005)] is the nondimensional property of the bulk electrolyte, where R denotes the universal gas constant; $K = \kappa h$ is the nondimensional channel height, where $\kappa = \sqrt{2z_v^2 e^2 N_A c_b/\varepsilon k_B T}$ is the Debye–Huckel parameter (Hunter 1981) with N_A the Avogadro's number. As such, the "figure of merit" Z is specified as

$$Z = \frac{M^2}{GS} = \frac{3(F_1 - 2\langle\zeta\rangle^*)^2}{2\left(F_2 - 2\zeta_D^{*2} + \beta K^2 F_3\right)} \tag{25}$$

The electrical double-layer potential is solved from the Poisson–Boltzmann equation (Hunter 1981)

$$\frac{d^2\Psi}{d\eta^2} = K^2 \sinh(\Psi) \tag{26}$$

Its boundary conditions are $\Psi(\pm 1) = \zeta_\pm^* = z_v e\zeta_\pm/k_BT$ where $\pm$ indicates the values at $\eta = +1$ and -1 (i.e., $y = +h$ and $-h$), respectively. In channels with weak double-layer overlapping (more specifically, $K \geq 2$), the solution to Eq. 26 may be expressed as (Russel et al. 1989; Garcia et al. 2005)

$$\Psi = 4\tanh^{-1}\left\{\tanh\left(\frac{\zeta_+^*}{4}\right)\exp[-K(1-\eta)]\right\} + 4\tanh^{-1}\left\{\tanh\left(\frac{\zeta_-^*}{4}\right)\exp[-K(1+\eta)]\right\} \tag{27}$$

4 Results and discussion

By using the above approach, the dependences of streaming effects and flow rate-modified streaming effects on surface heterogeneity in a two-section slit channel are examined and compared below. Each section is $w = 100$ μm wide and $l = 5$ mm long, while its half height h is varied to study the size effects. As illustrated in Fig. 2, the heterogeneity (displayed in black) may be distributed in a symmetric (Fig. 2a) or asymmetric manner (Fig. 2b). For each pattern, the direction of surface charge variations, $\hat{q}$, may be parallel or perpendicular to the flow direction (as indicated by the applied pressure gradient ∇p, see also Fig. 1). In all cases, the homogeneous surface (displayed in white in Fig. 2) of $\zeta_0 = -100$ mV and the heterogeneity of ζ_h varying from -100 to $+100$ mV are considered. Although the two sections in Fig. 2 are assumed to have equal dimensions, it is important to note that the proposed approach is also capable of estimating the streaming effects in channels with heterogeneity of variable coverage. The KCl aqueous solution of $c_b = 0.01$ mM is selected as the electrolyte. Its properties are assumed identical

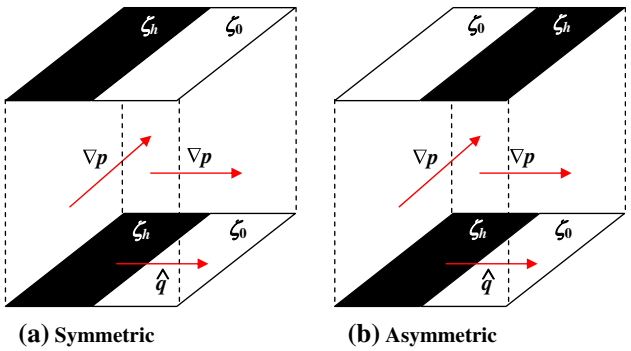

Fig. 2 Scheme of a two-section heterogeneous microchannel with (**a**) symmetrically and (**b**) asymmetrically distributed heterogeneity. The zeta potential of the homogeneous surface (in *white*) is $\zeta_0 = -100$ mV, while that of the heterogeneity (in *black*), ζ_h, may vary from -100 mV to $+100$ mV. The direction of the surface charge variations $\hat{q}$ may be parallel or perpendicular to the applied pressure gradient ∇p (i.e., the flow direction)

to pure water other than the molar conductivity, specifically including viscosity $\mu = 0.9 \times 10^{-3}$ kg m^{-1} s^{-1}, fluid permittivity $\varepsilon = 79 \times 8.854 \times 10^{-12}$ C V^{-1} m^{-1}, molar conductivity $\Lambda = 0.015$ S m^2 mol^{-1}, fluid temperature $T = 298$ K (van der Heyden et al. 2007).

To validate the presented thermo-electro-hydrodynamic approach, we have compared with Erickson and Li's (2001) numerical simulations the streaming potential and streaming current in a slit channel with stripwise heterogeneities parallel to the flow axis, i.e., $\hat{q} \perp \nabla$ in this context. Using the same channel and fluid properties, our analytical model predicts the streaming effects in close agreement with Erickson and Li's simulations. The discrepancy is mainly attributed to the approximate solution, i.e., Eq. 27, to the Poisson–Boltzmann equation, which becomes less accurate at higher zeta potentials (Russel et al. 1989).

For heterogeneous channels with $\hat{q} \parallel \nabla p$,, Fig. 3 compares streaming potential $\phi_{sp,\parallel}$ (Fig. 3a) and flow rate-modified streaming potential $\phi_{Q,\parallel}$ (Fig. 3b) when the heterogeneity is symmetrically (solid lines, refer to Fig. 2a) and asymmetrically (dashed lines, refer to Fig. 2b) distributed. Note that both quantities have been normalized by their respective values in a homogeneous microchannel ($\zeta_+ = \zeta_- = -100$ mV). Three different values of channel height, i.e., $K = 8$, 20 and 50, are considered. Apparently, streaming potential is sensitive to the arrangement of heterogeneity, especially in smaller microchannels (or at smaller K values). For both arrangements, the normalized streaming potential decreases from 1 to 0 but in dissimilar trends when the heterogeneous zeta potential ζ_h varies from -100 mV (virtually homogeneous) to $+100$ mV (overall neutral). Moreover, all curves deviate from the linear assumption (dashed-dotted line) or thin double-layer (TDL) approximation, though the discrepancy may be viewed

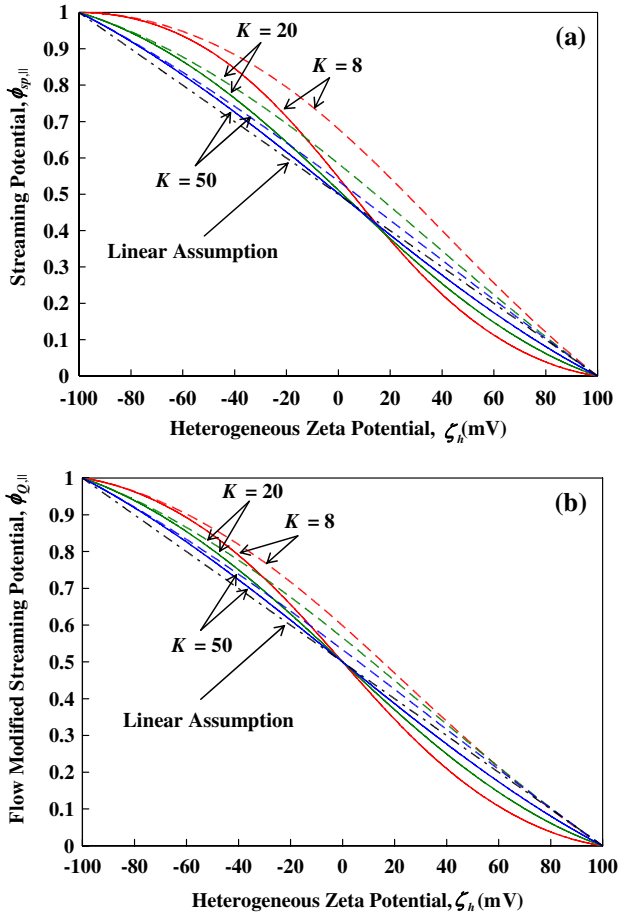

Fig. 3 Comparison of (**a**) streaming potential $\phi_{sp,\parallel}$ and (**b**) flow rate-modified streaming potential $\phi_{Q,\parallel}$ in a two-section heterogeneous microchannel with $\hat{q} \parallel \nabla p$, where the heterogeneity is symmetrically (*solid lines*) and asymmetrically (*dashed lines*) distributed. Both quantities have been normalized by their respective values in a homogeneous microchannel

negligible at $K > 50$. This approximation assumes an electroosmotic slip velocity on solid walls instead of the conventional no-slip condition, so that the solution of double-layer potential is avoided (Li 2004). Hence, the streaming potential is reduced to (Hunter 1981; Anderson and Idol 1985)

$$\phi_{sp,TDL} = \frac{\varepsilon\langle\zeta\rangle}{c_b\Lambda\mu}\Delta p \tag{28}$$

which is independent of the heterogeneous pattern (i.e., symmetric or asymmetric, $\hat{q} \parallel \nabla p$ or $\hat{q} \perp \nabla p$).

Equation 28 also implies that only at large K (e.g., $K > 50$) can the streaming potential in a homogeneous microchannel [i.e., $\zeta_+ = \zeta_- = \zeta$ in Eq. 19], which is $\phi_{sp} = M(-\Delta p)/S$ as seen in Eq. 2, be proportional to its zeta potential. This is because the phenomenological coefficients M in Eq. 22 and S in Eq. 23 are both nonlinear functions of ζ, particularly complex for S. In channels with large K values, where the thin double-layer approximation is valid, S is reduced to purely the electrical conductance of the electrolyte while M becomes proportional to the zeta potential. As for the flow rate-modified streaming potential in Fig. 3b, it follows the linear assumption in a better agreement than does the traditional streaming potential in Fig. 3a. Moreover, the dependence of the flow rate-modified streaming potential on the heterogeneous pattern also becomes weaker. This better consistency with the linear assumption may be attributed to the following: mathematically, the fewer terms related to zeta potential in $\phi_{Q,\parallel}$ than in $\phi_{sp,\parallel}$ (compare Eq. 7 with Eq. 5) and physically, the elimination of electrokinetic flow effects. This explanation also applies to the streaming potential when $\hat{q} \perp \nabla p$ (compare Eq. 15 with Eq. 13) and as well the streaming current case (compare Eqs. 10 and 18 with Eqs. 8 and 16, respectively).

Still in heterogeneous channels with $\hat{q} \parallel \nabla p$, Fig. 4 shows the comparison of streaming current $I_{sc,\parallel}$ (Fig. 4a) and flow rate-modified streaming current $I_{Q,\parallel}$ (Fig. 4b) when the heterogeneity is symmetrically (solid lines) and asymmetrically (dashed lines) distributed. Similarly, both quantities have been normalized by their respective values in a homogeneous microchannel. For a symmetric heterogeneous pattern, the decrease of streaming current with the rise of the heterogeneous zeta potential deviates from the linear assumption (dashed-dotted line), especially in smaller channels. Analogous to streaming potential, the linear prediction of streaming current is given by (Hunter 1981; Brunet and Ajdari 2006)

$$I_{sc,TDL} = -\frac{2\varepsilon hw\langle\zeta\rangle}{\mu l}\Delta p \tag{29}$$

which is again independent of the heterogeneous pattern. For an asymmetric heterogeneous pattern, however, all the three curves at different K values seem to agree well with the linear prediction in Fig. 4a. These different trends indicate that streaming current measurements are also dependent on the arrangement of heterogeneity, and may provide erroneous results if the linear relation is still assumed. As compared to the streaming current, the curves of the flow-modified streaming current in Fig. 4b approach closer to the linear prediction (dashed-dotted line). Such improvement is, however, not as obvious as that of the flow rate-modified streaming potential in Fig. 3.

For heterogeneous channels with $\hat{q} \perp \nabla p$, Fig. 5 compares streaming potential $\phi_{sp,\perp}$ (Fig. 5a) and flow rate-modified streaming potential $\phi_{Q,\perp}$ (Fig. 5b) when the heterogeneity is symmetrically (solid lines) and asymmetrically (dashed lines) distributed. Unlike that in channels with $\hat{q} \parallel \nabla p$ (see Fig. 3), streaming potential in this situation varies slightly with the arrangement of heterogeneity at variable K values. This result has been predicted

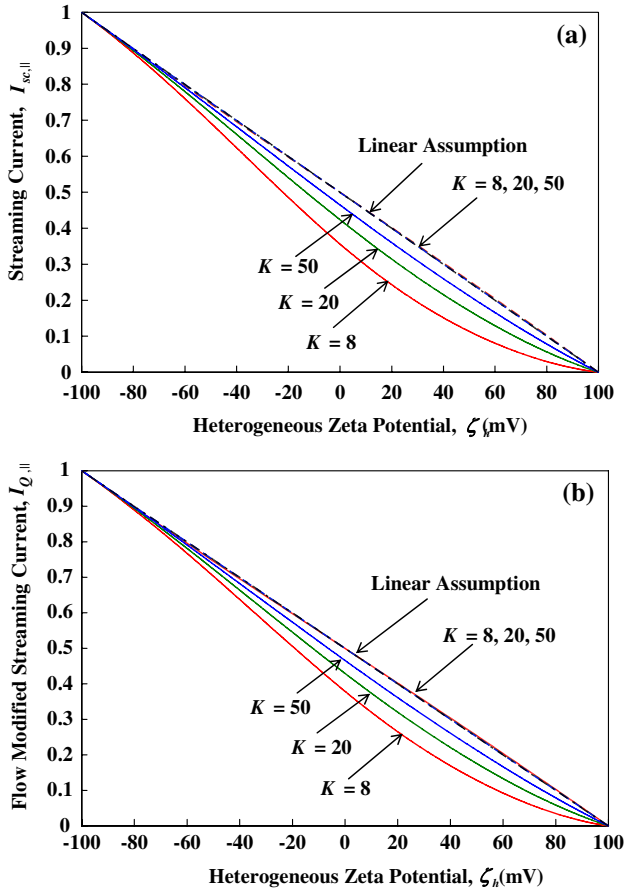

Fig. 4 Comparison of (**a**) streaming current $I_{sc,\parallel}$ and (**b**) flow rate-modified streaming current $I_{Q,\parallel}$ in a two-section heterogeneous microchannel with $\hat{q} \parallel \nabla p$, where the heterogeneity is symmetrically (*solid lines*) and asymmetrically (*dashed lines*) distributed. Both quantities have been normalized by their respective values in a homogeneous microchannel

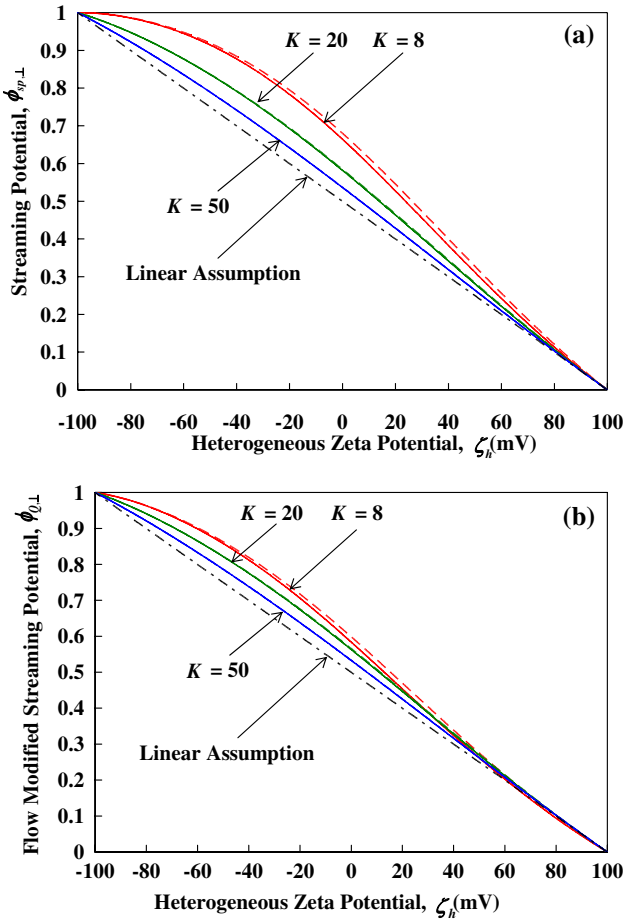

Fig. 5 Comparison of (**a**) streaming potential $\phi_{sp,\perp}$ and (**b**) flow rate-modified streaming potential $\phi_{Q,\perp}$ in a two-section heterogeneous channel with $\hat{q} \perp \nabla p$, where the heterogeneity is symmetrically (*solid lines*) and asymmetrically (*dashed lines*) distributed. Both quantities have been normalized by their respective values in a homogeneous microchannel

recently in Erickson and Li's (2001) numerical simulations. Also predicted in their paper is that the streaming potential differs from the linear assumption (dashed-dotted line), which is apparent in Fig. 5a. This deviation still exists in the flow rate-modified streaming potential (see Fig. 5b), where the electrokinetic flow effects have been neutralized. However, the flow rate-modified streaming potential does provide more consistent results with the linear assumption (dashed-dotted line), especially in smaller microchannels where the electrokinetic flow effects are more pronounced.

In heterogeneous channels with $\hat{q} \perp \nabla p$, streaming current is unaffected by the distribution of heterogeneity, because the electrokinetic flow effects do not exist. Hence, both the streaming current and the flow rate-modified streaming current follow the linear prediction with only minor deviations. This result, which has been discussed in Erickson and Li's (2001) paper, is readily anticipated from Eqs. 16 and 18, where the only zeta potential-associated terms M_i are involved in both equations.

5 Conclusions

We have developed an analytical model to study the streaming potential and streaming current in heterogeneous microchannels. The heterogeneities may be symmetrically or asymmetrically distributed parallel or perpendicular to the pressure-driven flow direction. Flow rate-modified streaming effects have been defined to eliminate the possible influence of electrokinetic flow on the traditional streaming potential and streaming current measurements. The results have demonstrated that these new streaming effects provide more consistent results with the generally assumed linear relationships than do the traditional ones. As both the streaming effects and the flow rate are readily measurable, the flow-rate modified streaming effects can serve as an alternative while more reliable means to characterize heterogeneous surfaces than do the traditional streaming effects, especially in channels with small K

values. Additionally, our results show that the flow rate-modified streaming effects and the traditional streaming effects as well are dependent on the heterogeneous pattern (i.e., symmetric or asymmetric, parallel or perpendicular to the flow axis) unless in channels with large K.

Acknowledgments Financial support from Clemson University through a start-up package and a Research Investment Initiative Fund to X.X. is gratefully acknowledged.

References

Ajdari A (1995) Electroosmosis on inhomogeneously charged surfaces. Phys Rev Lett 75:755–758

Ajdari A (1996) Generation of transverse fluid currents and forces by an electric field: electro-osmosis on charge-modulated and undulated surfaces. Phys Rev E 53:4996–5005

Anderson JL, Idol WK (1985) Electroosmosis through pores with nonuniformly charged walls. Chem Eng Commun 38:93–106

Berli CLA (2007) Theoretical modeling of electrokinetic flow in microchannel networks. Colloid Surf A 301:271–280

Berli CLA (2008) Equivalent circuit modeling of electrokinetically driven analytical microsystems. Microfluid Nanofluid 4:391–399

Biddiss E, Erickson D, Li D (2004) Heterogeneous surface charge enhanced micromixing for electrokinetic flows. Anal Chem 76:3208–3213

Brunet E, Ajdari A (2004) Generalized Onsager relations for electrokinetic effects in anisotropic and heterogeneous geometries. Phys Rev E 69:016306

Brunet E, Ajdari A (2006) A thin double layer approximation to describe streaming current fields in complex geometries: analytical framework and application to microfluidics. Phys Rev E 73:056306

Chein R, Liao J (2007) Analysis of electrokinetic pumping efficiency in capillary tubes. Electrophoresis 28:635–643

Davidson C, Xuan X (2008a) Effects of Stern layer conductance on electrokinetic energy conversion in nanofluidic channels. Electrophoresis 29:1125–1130

Davidson C, Xuan X (2008b) Electrokinetic energy conversion in slip nanochannels. J Power Sources 179:297–300

de Groot SR (1952) Thermodynamics of irreversible processes. Interscience, New York

Elgersma AV, Zsom RLJ, Lyklema J, Norde W (1992) Kinetics of single and competitive protein adsorption studied by reflectometry and streaming potential measurements. Colloid Surf 65:17–28

Erickson D, Li D (2001) Streaming potential and streaming current methods for characterizing heterogeneous solid surfaces. J Colloid Interface Sci 237:283–289

Erickson D, Li D (2002) Influence of surface heterogeneity on electrokinetically driven microfluidic mixing. Langmuir 18:1883–1892

Garcia AL, Ista LK, Petsev DN et al (2005) Electrokinetic molecular separation in nanoscale fluidic channels. Lab Chip 5:1271–1276

Griffiths SK, Nilson RH (2005) The efficiency of electrokinetic pumping at a condition of maximum work. Electrophoresis 26:351–361

Herr AE, Molho JI, Santiago JG, Mungal MG, Kenny TW, Garguilo MG (2000) Electroosmotic capillary flow with nonuniform zeta potential. Anal Chem 72:1053–1057

Hunter RJ (1981) Zeta potential in colloid science, principles and applications. Academic Press, New York

Li D (2001) Electro-viscous effects on pressure-driven liquid flow in microchannels. Colloid Surf A 191:35–57

Li D (2004) Electrokinetics in microfluidics. Elsevier, Burlington

Morrison FA, Osterle JF (1965) Electrokinetic energy conversion in untrafine capillaries. J Chem Phys 43:2111–2115

Norde W, Rouwendal E (1990) Streaming potential measurements as a tool to study protein adsorption kinetics. J Colloid Interface Sci 139:169–176

Ren L, Li D (2001) Electro-osmotic flow in heterogeneous microchannels. J Colloid Interface Sci 243:255–261

Ren Y, Stein D (2008) Slip enhanced electrokinetic energy conversion in nanofluidic channels. Nanotechnology 19:195707

Russel WB, Saville DA, Schowalter WR (1989) Colloidal dispersions. Cambridge University Press, Cambridge

Squires TM, Quake SR (2005) Microfluidics: fluid physics at the nanoliter scale. Rev Mod Phys 7:977–1026

Stroock AD, Weck M, Chiu DT, Huck WT, Kenis PJ, Ismagilov RF, Whitesides GM (2000) Patterning electroosmotic flows with patterned surface charge. Phys Rev Lett 84:3314–3317

Towns JK, Regnier FE (1991) Capillary electrophoretic separations of proteins using nonionic surfactant coatings. Anal Chem 63:1126–1132

Towns JK, Regnier FE (1992) Impact of polycation adsorption on efficiency and electroosmotically driven transport in capillary electrophoresis. Anal Chem 64:2473–2478

van der Heyden FHJ, Bonthius DJ, Stein D, Meyer C, Dekker C (2006) Electrokinetic energy conversion efficiency in nanofluidic channels. Nano Lett 6:2232–2237

van der Heyden FHJ, Bonthius DJ, Stein D, Meyer C, Dekker C (2007) Power generation by pressure-driven transport of ions in nanofluidic channels. Nano Lett 7:1022–1025

Werner C, Korber H, Zimmermann R, Dukhin S, Jacobasch H (1998) Extended electrokinetic characterization of flat solid surfaces. J Colloid Interface Sci 208:329

Werner C, Konig U, Augsburg A, Arnhold C, Korber H, Zimmermann R, Jacobasch HJ (1999) Electrokinetic surface characterization of biomedical polymers—a survey. Colloid Surf A 159:519–529

Xuan X, Li D (2004) Analysis of electrokinetic flow in microfluidic networks. J Micromech Microeng 14:290–298

Xuan X, Li D (2006) Thermodynamic analysis of electrokinetic energy conversion. J Power Sources 156:677–684

Xuan X (2008) Streaming potential and electroviscous effect in heterogeneous microchannels. Microfluid Nanofluid 4:457–462

Zembala M, Adamczyk Z (2000) Measurements of streaming potential for mica covered by colloid particles. Langmuir 16:1593–1601

Zembala M (2004) Electrokinetics of heterogeneous interfaces. Adv Colloid Surf Sci 112:59–92